Microporous Membrane Blood Oxygenators

S. R. Wickramasinghe, B. Han, J. D. Garcia, and R. Specht
Dept. of Chemical Engineering, Colorado State University, Fort Collins, CO 80523

DOI 10.1002/aic.10327
Published online January 14, 2005 in Wiley InterScience (www.interscience.wiley.com).

Extracorporeal blood oxygenators are used to oxygenate blood during open-heart surgery. Hydrophobic microporous flat-sheet or hollow-fiber membranes are used to separate blood and gas phases. Oxygen diffuses from the gas phase through the gas-filled membrane pores into the blood. Mass-transfer and friction-factor correlations have been developed for flat-sheet and hollow-fiber blood oxygenators. Generalized Graetz, Reynolds, and Schmidt numbers are used in these correlations to account for the shear-thinning behavior of blood. Because oxygen not only dissolves in plasma but also binds to hemoglobin, a mass-transfer enhancement factor based on film theory has been developed to account for oxygen binding to hemoglobin. Experimental results for oxygen transfer to bovine blood and both non-Newtonian and Newtonian blood analogue fluids indicate that the correlations developed may be used to predict the performance of a blood oxygenator based on results for an experimentally simple system such as the oxygenation of deionized water. © 2005 American Institute of Chemical Engineers *AIChE J,* 51: 656–670, 2005

Keywords: blood oxygenators, friction factor, mass transfer, microporous membranes

Introduction

Extracorporeal blood oxygenators (BOs) have been used for over 50 years to oxygenate a patient's blood during open-heart surgery. Today over 99% of BOs sold in the United States contain microporous membranes. Flat sheets and hollow fibers are used, although the latter geometry is more popular. Devices with very low membrane surface areas (such as Sarns Turbo and Cobe Optima have surface areas of 1.9 and 1.7 m^2, respectively) have been built using carefully spaced mats of woven hollow fibers (Baurmeister, 1990, 1992). These woven hollow fibers provide uniform flow channels to minimize channeling of the blood.

More recently, computational fluid dynamics (CFD) models have been developed to guide the design of new BOs (Bludszuweit, 1997; Gartner et al., 2000; Goodin et al., 1994). Although these models are helpful, further experimental studies are still necessary. Conducting experiments using human blood is costly and time consuming. A number of safety procedures are required when using human blood to minimize the risk of transmission of pathogens from the blood being tested to the operator. Consequently, sheep and bovine blood have been used as models for human blood (Bellhouse et al., 1973; Mockros and Leonard, 1985; Vaslef et al., 1994). Although animal blood is far safer than human blood, the large amount of biological variability between units of blood can make comparison of experimental results for different units of blood difficult in research and development studies. For instance the percentage by volume of red blood cells (hematocrit) of human blood has been shown to vary from 20 to >40% (Altman and Dittmer, 1971; Dittmer and Grebe, 1959). Similarly for cattle and sheep the hematocrit has been shown to vary from 30 to 40%. In addition, the physical condition of the subject could affect the properties of red blood cells such as their flexibility.

The aim of the study reported herein is to develop mass-transfer and friction-factor correlations for commercially available BOs that may be used to predict the rate of gas transfer and the pressure drop for blood, using nonbiological, nonpathogenic blood analogue fluids. Blood is rheologically complex. It is a shear-thinning viscoelastic fluid (Zydney et al., 1991). Blood shows thixotropic properties arising from its slow recovery from shear degradation and displays an apparent yield stress (Thurston, 1979).

Correspondence concerning this article should be addressed to S. R. Wickramasinghe at Max-Plank-Institut für Dynamik komplexer technischer Systeme, Sandtorstraβe 1, 39106 Magdeburg, Germany.

Table 1. Mass-Transfer and Friction-Factor Correlations for Flat-Sheet and Hollow-Fiber BOs Using Newtonian Blood Analogue Liquids

	Flow in Flat-Sheet BOs (Goerke et al., 2002)	Flow Across Hollow-Fiber BOs (Goerke et al., 2002; Wickramasinghe et al., 2002a)	Comments
Mass transfer	$K = \frac{Q}{A}\ln\left(\frac{C_I - C^*}{C_O - C^*}\right)$	$K = \frac{Q}{A}\ln\left(\frac{C_I - C^*}{C_O - C^*}\right)$	For flow in polydisperse channels, mass transfer can be compromised; use average mass-transfer coefficient in mass-transfer correlations
	Average mass transfer coefficient: $\langle K\rangle = K\left[1 - \left(\frac{9KA}{Q} - 3\right)\varepsilon_0^2 + \cdots\right]$		
	Mass transfer correlation: $\mathrm{Sh} = 0.5\,\mathrm{Gr}$ $(0.5 < \mathrm{Gr} < 10)$; $\mathrm{Sh} = 3.0\,\mathrm{Gr}^{0.33}$ $(10 < \mathrm{Gr} < 500)$	Mass transfer correlation: $\mathrm{Sh} = 0.8\mathrm{Re}^{0.59}\mathrm{Sc}^{0.33}$	Experimentally determined correlations for BOs
Friction factor	Friction factor: $f = \frac{B}{L}\frac{\Delta P}{\frac{1}{2}\rho u^2}$	Friction factor: $f = \frac{d_e \Delta P}{4L_0 \frac{1}{2}\rho u^2}$	Based on the definition of the friction factor
	Friction factor correlation: $f = 24/\mathrm{Re}$	Friction factor correlation: $f = 260\mathrm{Re}^{-1.1}$ $0.1 < \mathrm{Re} < 5$; $f = 100\mathrm{Re}^{-0.5}$ $5 < \mathrm{Re} < 100$	Experimentally determined correlations for BOs

Blood rheology is often described in terms of two basic phenomena (Chien et al., 1966): red cell deformation and red cell aggregation. During cardiopulmonary bypass, addition of fluids such as anticoagulants leads to a reduction in the hematocrit (percentage by volume of red blood cells) of the blood. Typically, the hematocrit is <35% (Voorhees and Brian, 1996). Under these conditions, the elastic properties of the blood do not play a significant role in its flow behavior (Brookshier and Tarbell, 1993). Further, because of the low hematocrit, cell–cell interactions are likely to be less important. In microporous-membrane BOs the average shear stress on the blood is about 5–20 Pa (Voorhees and Brian, 1996). Under these conditions blood may be modeled as a shear-thinning fluid (Zydney et al., 1991). Consequently, the friction-factor correlations developed for blood analogue fluids must account for the shear-thinning behavior of blood.

In human and animal blood, oxygen diffuses into the plasma and binds to hemoglobin, whereas in the nonbiological blood analogue fluids studied here, no reaction of the dissolved oxygen occurs. Thus, to predict the rate of gas transfer to and from blood, the effects of the oxygen hemoglobin reaction must be accounted for in the mass-transfer correlation developed for the blood analogue fluids.

Predicting the rate of gas transfer and the pressure drop for blood flowing through a BO using nonbiological, nonpathogenic fluids, could lead to significant cost savings when designing new BOs. Initial experiments conducted to screen potential new BO designs may be carried out using blood analogue fluids. Further, the use of nonbiological, nonpathogenic fluids to predict the rate of gas transfer and the pressure drop for blood could lead to the development of a valuable quality assurance/quality control method.

Experimentally determined rates of oxygen transfer to and from blood analogue fluids and bovine blood are presented for commercially available flat-sheet and hollow-fiber BOs. The gas phase consisted of pure oxygen or nitrogen. The pressure drop for liquid flow through these devices has also been measured. Mass-transfer and friction-factor correlations have been developed that account for the shear-thinning behavior and the oxygen hemoglobin reaction that occur in bovine blood. Based on film theory, a mass-transfer enhancement factor has been developed to account for the increased rate of oxygen transfer arising from the oxygen hemoglobin reaction.

Theory

Newtonian blood analogue fluids

Newtonian blood analogue fluids, consisting of deionized water and mixtures of glycerol and deionized water, have been used to develop mass-transfer and friction-factor correlations (Goerke et al., 2002; Wickramasinghe et al., 2002a). Because the mass-transfer and friction-factor correlations for bovine blood are based on these results, the results are summarized in Table 1 and briefly described below.

The transfer of oxygen to Newtonian blood analogue fluids may be described by the following equation (Cussler, 1997)

$$N = K\Delta C \tag{1}$$

where N is the total molar flux, ΔC is the overall concentration difference, and K is the overall average mass-transfer coefficient. A mass balance over the liquid phase results in the following expression for the overall average mass-transfer coefficient

$$K = \frac{Q}{A}\int_{C_I}^{C_O}\frac{dC}{C^* - C} \tag{2}$$

where Q is the fluid flow rate; A is the membrane surface area; and C_I, C_O, and C^* are the inlet and outlet oxygen concentrations in the fluid and the oxygen concentration in the fluid if it were in equilibrium with the gas phase (pure oxygen or nitrogen), respectively (Goerke et al., 2002; Sirkar, 1992). Integration of Eq. 2 results in the following equation, which may be

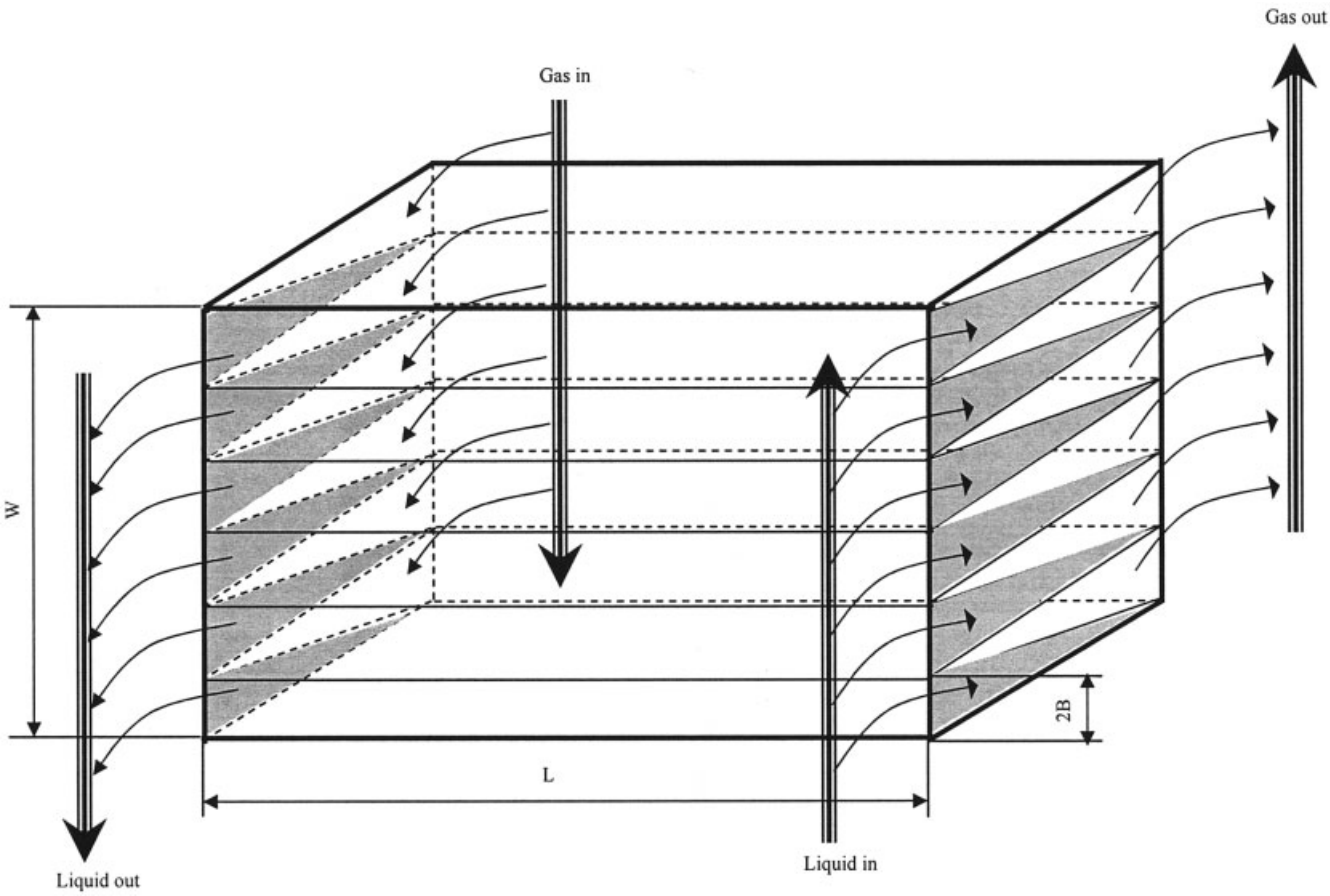

Figure 1. Flat-sheet BOs.

The liquid and gas phases flow in alternating approximately rectangular channels separated by a flat-sheet membrane.

used to calculate the mass-transfer coefficient from the experimentally determined oxygen concentration in the liquid phase

$$K = \frac{Q}{A} \ln\left(\frac{C_I - C^*}{C_O - C^*}\right) \tag{3}$$

For blood oxygenation using microporous membranes, the liquid side concentration boundary layer represents the major resistance to gas transfer (Goerke et al., 2002; Yang and Cussler, 1986; Zhang and Cussler, 1985a,b). Consequently the overall average mass-transfer coefficient may be approximated by the liquid side mass-transfer coefficient. Experimentally this means that the overall average mass-transfer coefficient is independent of gas flow rate. Table 1 summarizes experimentally determined mass-transfer and friction-factor correlations for Newtonian fluids flowing in flat-sheet and hollow-fiber BOs.

Flat-Sheet BOs. In flat-sheet BOs, as shown in Figure 1, the liquid flows in approximately rectangular channels. Goerke et al. (2002) showed that slight variations in the thickness of these channels leads to compromised mass transfer. Assuming that the variation in channel thickness may be represented by a normal distribution, the average mass-transfer coefficient, $\langle K \rangle$, for flow in polydisperse channels is given by the expression

$$\langle K \rangle = K\left[1 - \left(\frac{9KA}{Q} - 3\right)\varepsilon_0^2 + \cdots\right] \tag{4}$$

where K is the mass-transfer coefficient for flow in uniform channels and ε_0 is the standard deviation divided by the mean of the distribution of channel thickness.

Graetz (1883, 1885) derived an expression for the rate of heat transfer in laminar flow to the walls of a round tube. Lévêque (1928) showed that for the entrance region of the tube where the thermal boundary layer is thin, a simpler solution is obtained. The mass-transfer analogue to the Lévêque equation for flow in rectangular ducts is given by (Shah and London, 1974)

$$\mathrm{Sh} = 6.4\mathrm{Gr}^{0.33} \tag{5}$$

where Sh is the Sherwood number and Gr is the Graetz number, defined, respectively, as

$$\mathrm{Sh} = \frac{K(4B)}{D} \tag{6}$$

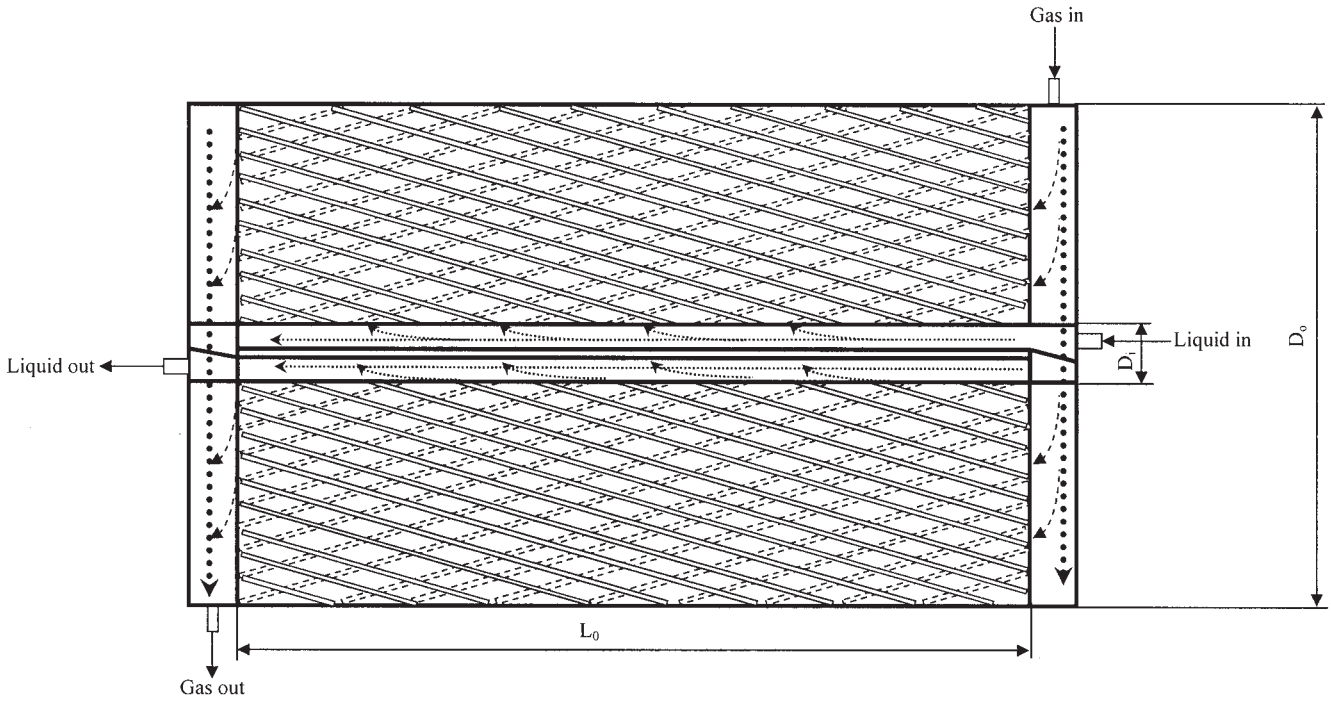

Figure 2. Schematic representation of hollow-fiber BOs.

The liquid phase flows outside and across the fibers, whereas the gas flows inside the fibers.

$$\mathrm{Gr} = \frac{(4B)^2 u}{DL} \tag{7}$$

In Eqs. 6 and 7 B is the average half-thickness of the rectangular channels, D is the diffusion coefficient of oxygen, u is the liquid velocity, and L is the length of the rectangular channel. The mass-transfer coefficient for flat-sheet BOs may be predicted by replacing the mass-transfer coefficient K in Eq. 6 by the average mass-transfer coefficient given by Eq. 4.

For laminar flow in thin rectangular ducts, Darby (1996) showed that the friction factor may be approximated by

$$f = \frac{24}{\mathrm{Re}} \tag{8}$$

where Re is the Reynolds number, which is defined as

$$\mathrm{Re} = \frac{u(4B)}{\nu} \tag{9}$$

where ν is the kinematic viscosity of the liquid phase.

Hollow-Fiber BOs. For flow across mats of woven hollow fibers (Figure 2) the mass-transfer correlation has the form

$$\mathrm{Sh} = a\mathrm{Re}^b\mathrm{Sc}^c \tag{10}$$

where Sc is the Schmidt number and a, b, and c are empirical constants. Wickramasinghe et al. (2002a) determined the values for the empirical constants and thus developed the following mass-transfer correlation:

$$\mathrm{Sh} = 0.8\mathrm{Re}^{0.59}\mathrm{Sc}^{0.33} \tag{11}$$

The Schmidt number is defined as

$$\mathrm{Sc} = \frac{\nu}{D} \tag{12}$$

For flow across woven hollow fibers, the Sherwood and Reynolds numbers are defined, respectively, as

$$\mathrm{Sh} = \frac{Kd_e}{D} \tag{13}$$

$$\mathrm{Re} = \frac{ud_e}{\nu} \tag{14}$$

where d_e is the equivalent diameter, defined as (Wickramasinghe et al., 2002a)

$$d_e = \frac{\varepsilon}{1-\varepsilon} d_0 \tag{15}$$

In Eq. 15, ε is the void fraction defined as the ratio of the empty volume within the mass-transfer chamber to the total volume of the mass-transfer chamber and d_0 is the outside diameter of the hollow fibers.

Wickramasinghe et al. (2002a) determined the following experimental friction-factor correlations for flow across woven hollow fibers:

$$f = 260\mathrm{Re}^{-1.1} \qquad 0.1 < \mathrm{Re} < 5 \tag{16}$$

$$f = 100\mathrm{Re}^{-0.5} \qquad 5 < \mathrm{Re} < 100 \tag{17}$$

Non-Newtonian blood analogue fluids

Few mass-transfer and friction-factor correlations are available for non-Newtonian blood analogue fluids. Here, non-Newtonian blood analogue fluids consisting of glycerol–water mixtures containing small amounts of xantham gum have been prepared and rheologically characterized. These fluids were then used as the liquid phase in flat-sheet and hollow-fiber BOs. Wickramasinghe et al. (2002b) showed that the resulting shear-thinning fluids may be used to model the rheological behavior of blood in a BO. The rheological behavior of these blood analogue fluids is described using the following power-law model

$$\tau = m\dot{\gamma}^n \tag{18}$$

where τ is the shear stress, $\dot{\gamma}$ is the shear rate, and m and n are the power-law parameters. Generalized Reynolds and Schmidt number, Re_p and Sc_p for power-law fluids, may be defined as (Wickramasinghe et al., 2002b)

$$\mathrm{Re}_p = \frac{\rho u_p d}{\mu_p} = \left(\frac{d^n u^{2-n}\rho}{m}\right)8\left(\frac{n}{6n+2}\right) \tag{19}$$

$$\mathrm{Sc}_p = \frac{\nu_p}{D} = \frac{m}{\rho D}\left(\frac{8\nu}{d}\frac{3n+1}{4n}\right)^{n-1} \tag{20}$$

where u_p is the average velocity of the shear-thinning fluid, which may be related to the average velocity of a Newtonian fluid by

$$u_p = \frac{4n}{1+3n}u \tag{21}$$

Wickramasinghe et al. (2002b) showed that by replacing the Newtonian Reynolds and Schmidt numbers (Re and Sc) by their power-law equivalents (Re_p and Sc_p), Eq. 11 predicted the mass-transfer coefficient for flow across bundles of woven hollow fibers. These results are extended here to predict the mass-transfer coefficient for flow in rectangular channels. In addition, friction-factor correlations for non-Newtonian fluids flowing across bundles of hollow fibers and in rectangular channels have also been determined.

Here, analogous to Eqs. 19 and 20, generalized Graetz and Reynolds numbers for the power-law fluids flowing in flat-sheet BOs are defined as

$$\mathrm{Gr}_p = \frac{(4B)^2 u_p}{DL} = \frac{(4B)^2}{DL}\left(\frac{4n}{1+3n}\right)u \tag{22}$$

$$\mathrm{Re}_p = \frac{u_p(4B)}{\nu_p} = \left(\frac{(4B)^n u^{2-n}\rho}{m}\right)8\left(\frac{n}{6n+2}\right) \tag{23}$$

Equation 5 may be used to predict the mass-transfer coefficient for power-law fluids flowing in flat-sheet BOs, providing the Graetz number Gr is replaced by the generalized Graetz number Gr_p, given by Eq. 22. Equation 4 is used to account for the effect of slight variations in the liquid flow channel thickness.

The friction factor for flow in flat-sheet BOs may be predicted using Eq. 8, providing the Reynolds number is replaced by Re_p, given in Eq. 23. Similarly the friction factor for flow across bundles of woven hollow fibers may be predicted using Eqs. 16 and 17, providing the Reynolds number is replaced by Re_p, given by Eq. 19.

Bovine blood

The rheological behavior of bovine blood may be modeled using the power law as described above. However, in the case of bovine blood the reaction of dissolved oxygen with the hemoglobin present in the blood will lead to an enhanced rate of mass transfer compared to nonreactive blood analogue fluids. A general enhancement factor to the mass-transfer coefficient may be calculated based on film theory (Nernst, 1904).

The hemoglobin molecule is a globular protein composed of four polypeptide chains each containing a heme group. The oxygen-binding curve for hemoglobin (that is, percentage of saturation of hemoglobin as a function of oxygen partial pressure) has a sigmoidal shape (Antonini and Brunori, 1975). The shape of the binding curve indicates the existence of functional interactions between the heme units.

The oxygen binding curve may be described empirically, assuming the reaction between hemoglobin and oxygen is given by the following expression

$$\mathrm{Hb} + n\mathrm{O}_2 \underset{k_{-1}}{\overset{k_1}{\longleftrightarrow}} \mathrm{Hb(O_2)}_n \tag{24}$$

where n is a measure of cooperativity between heme units (Ranney and Sharma, 2001). For bovine blood, $n = 2.85$, whereas for human blood, $n = 2.7$.

An apparent equilibrium constant K_E, based on Eq. 24, may be defined as

$$K_E = \frac{k_1}{k_{-1}} = \frac{[\mathrm{Hb(O_2)}_n]}{[\mathrm{Hb}][\mathrm{O_2}]^n} \tag{25}$$

where k_1 and k_{-1} are the forward and backward rate constants and $[\mathrm{Hb(O_2)}_n]$, [Hb], and $[\mathrm{O_2}]$ are the concentrations of oxygenated hemoglobin, nonoxygenated hemoglobin, and dissolved oxygen in the plasma, respectively.

The degree of oxygen saturation (oxyhemoglobin saturation) S is given by the ratio $[\mathrm{Hb(O_2)}_n]/[\mathrm{Hb}]_t$, where $[\mathrm{Hb}]_t$ is the total hemoglobin concentration (oxygenated and nonoxygenated) present. The degree of oxygen saturation is often described by the Hill equation (Goldstick, 1973; Hill, 1910; Vaslef, 1990)

$$S = \frac{[\mathrm{Hb(O_2)}_n]}{[\mathrm{Hb}]_t} = \frac{(P_{O_2}/P_{50})^n}{1+(P_{O_2}/P_{50})^n} \tag{26}$$

where P_{O_2} and P_{50} are the oxygen partial pressure and the oxygen partial pressure at 50% hemoglobin saturation. At pH 7.4 and 37°C, for bovine blood $P_{50} = 3870$ Pa, whereas for human blood, $P_{50} = 3550$ Pa (Mockros and Leonard, 1985). Equation 26 may be obtained from Eq. 25 if

$$K_E = \frac{1}{(\alpha P_{50})^n} \tag{27}$$

where α is the physical solubility of oxygen in blood.

Equation 25 may also be rewritten as

$$[Hb(O_2)_n] = \frac{K_E[Hb]_t[O_2]^n}{1 + K_E[O_2]^n} = \frac{[Hb]_t[O_2]^n}{K_D + [O_2]^n} \tag{28}$$

where $K_D = 1/K_E$. Equation 28 is the expression for the Freundlich–Langmuir isotherm (Liu, 1989; Suzuki, 1990; Yang and Chen, 2002), which is often used to fit data where ligand binding is characterized by nonindependent binding sites.

The rates of production of $[O_2]$, [Hb], and $[Hb(O_2)_n]$, arising from the reversible reaction between hemoglobin and oxygen, are given by the following expressions

$$\frac{1}{n}\frac{d[O_2]}{dt} = k_{-1}[Hb(O_2)_n] - k_1[Hb][O_2]^n \tag{29}$$

$$\frac{d[Hb]}{dt} = k_{-1}[Hb(O_2)_n] - k_1[Hb][O_2]^n \tag{30}$$

$$\frac{d[Hb(O_2)_n]}{dt} = -k_{-1}[Hb(O_2)_n] + k_1[Hb][O_2]^n \tag{31}$$

Here only the liquid side film is considered because the gas side resistance to mass transfer is negligible in BOs. Mass transfer by convection within the film is negligible. Further, there is no mass accumulation at any point within the film. Consequently, steady-state mass balances in the liquid film on $[O_2]$, [Hb], and $[Hb(O_2)_n]$ lead to the following equations (Bird et al., 2001; Cussler, 1997)

$$0 = \frac{\partial[O_2]}{\partial t} = D_{O_2}\frac{\partial^2([O_2])}{\partial x^2} + nk_{-1}[Hb(O_2)_n] - nk_1[Hb][O_2]^n \tag{32}$$

$$0 = \frac{\partial[Hb]}{\partial t} = D_{Hb}\frac{\partial^2([Hb])}{\partial x^2} + k_{-1}[Hb(O_2)_n] - k_1[Hb][O_2]^n \tag{33}$$

$$0 = \frac{\partial[Hb[O_2)_n]}{\partial t} = D_{Hb(O_2)_n}\frac{\partial^2([Hb(O_2)_n])}{\partial x^2} - k_{-1}[Hb(O_2)_n] + k_1[Hb][O_2]^n \tag{34}$$

Combining Eqs. 32 and 34 gives

$$0 = \frac{\partial[O_2]}{\partial t} + n\frac{\partial[Hb(O_2)_n]}{\partial t} = D_{O_2}\frac{\partial^2([O_2])}{\partial x^2} + nD_{Hb(O_2)_n}\frac{\partial^2([Hb(O_2)_n])}{\partial x^2} \tag{35}$$

Combining Eqs. 33 and 34 gives

$$0 = \frac{\partial[Hb]}{\partial t} + \frac{\partial[Hb(O_2)_n]}{\partial t} = D_{Hb}\frac{\partial^2([Hb])}{\partial x^2} + D_{Hb(O_2)_n}\frac{\partial^2([Hb(O_2)_n])}{\partial x^2} \tag{36}$$

The general solutions for Eqs. 35 and 36 are (Olander, 1960) as follows

$$D_{O_2}[O_2] + nD_{Hb(O_2)_n}[Hb(O_2)_n] = a_1x + a_2 \tag{37}$$

$$D_{Hb}[Hb] + D_{Hb(O_2)_n}[Hb(O_2)_n] = a_3x + a_4 \tag{38}$$

where a_1, a_2, a_3, and a_4 are empirical constants. Four boundary conditions are required. At the gas–liquid interface (surface of the membrane on the liquid side), $x = 0$. Here

$$[O_2] = [O_2]_0 \tag{39}$$

where $[O_2]_0$ is the dissolved oxygen concentration in the liquid phase that is in equilibrium with the gas-phase concentration. At the outer edge of the stagnant film, $x = \delta$. Here

$$[O_2] = [O_2]_\delta \tag{40}$$

$$[Hb] = [Hb]_\delta \tag{41}$$

where $[O_2]_\delta$ and $[Hb]_\delta$ are the same as the dissolved oxygen and nonoxygenated hemoglobin concentrations in the bulk liquid.

Neither hemoglobin nor oxygenated hemoglobin can leave the liquid phase. Thus the fourth boundary condition states that the flux of total hemoglobin is zero

$$D_{Hb}\frac{d([Hb])}{dx} + D_{Hb(O_2)_n}\frac{d([Hb(O_2)_n])}{dx} = 0 \tag{42}$$

The rate of oxygen transfer through the stagnant film is equal to the dissolved oxygen flux plus the oxygenated hemoglobin flux. Thus, the oxygen flux J is

$$J = -D_{O_2}\frac{d[O_2]}{dx} - nD_{Hb(O_2)_n}\frac{d[Hb(O_2)_n]}{dx} = -a_1 \tag{43}$$

Substituting Eqs. 25 and 37–42 into Eq. 43 results in

$$J = \frac{D_{O_2}}{\delta}([O_2]_0 - [O_2]_\delta)\left\{1 + \frac{nD_{Hb(O_2)_n}}{D_{O_2}} \times \frac{1}{1+\frac{D_{Hb(O_2)_n}}{D_{Hb}} K_E[O_2]_0^n} \frac{[O_2]_0^n - [O_2]_\delta^n}{[O_2]_0 - [O_2]_\delta} K_E[Hb]_\delta\right\} \quad (44)$$

In the absence of a chemical reaction between oxygen and hemoglobin, the oxygen flux J_0 is

$$J_0 = \frac{D_{O_2}}{\delta}([O_2]_0 - [O_2]_\delta) = k_0([O_2]_0 - [O_2]_\delta) \quad (45)$$

where k_0 is the mass-transfer coefficient in the absence of chemical reaction. Comparing Eqs. 44 and 45

$$k = k_0\left\{1 + \frac{nD_{Hb(O_2)_n}}{D_{O_2}} \times \frac{1}{1 + \frac{D_{Hb(O_2)_n}}{D_{Hb}} K_E[O_2]_0^n} \frac{[O_2]_0^n - [O_2]_\delta^n}{[O_2]_0 - [O_2]_\delta} K_E[Hb]_\delta\right\} = k_0 E \quad (46)$$

where the term within the braces is the enhancement factor E. If $n = 1$ the chemical reaction given by Eq. 24 has the form

$$Hb + O_2 \underset{k_{-1}}{\overset{k_1}{\longleftrightarrow}} Hb(O_2) \quad (47)$$

The mass-transfer coefficient becomes

$$k = k_0\left\{1 + \frac{D_{Hb(O_2)}}{D_{O_2}} \frac{1}{1 + \frac{D_{Hb(O_2)}}{D_{Hb}} K_E[O_2]_0} K_E[Hb]_\delta\right\} \quad (48)$$

where the enhancement factor is given by the term within the braces. This expression is identical to the enhancement factor given by Olander (1960) for a chemical reaction of the form given by Eq. 47.

The overall average mass-transfer coefficient in the BO may still be calculated from Eq. 2. However, in blood, oxygen is present in both dissolved and chemically reacted forms. Therefore, the oxygen concentration in blood is given by

$$C = C_C + C_P = \beta(Ht/100)S + \alpha P_{O_2} \quad (49)$$

where β is the maximum amount of oxygen that can combine with a unit volume of hemoglobin; and C_C and C_P are the oxygen concentration bound to hemoglobin and dissolved in the plasma, respectively. Therefore Eq. 2 can be rewritten as

$$K = \frac{Q}{A}\int_{C_{P,I}}^{C_{P,O}} \frac{dC}{(C^* - C_P)} = \frac{Q}{A}\int_{C_{P,I}}^{C_{P,O}} \frac{d[\beta(Ht/100)S + \alpha P_{O_2}]}{(C^* - C_P)} \quad (50)$$

where $C_{P,I}$ and $C_{P,O}$ are the oxygen concentration dissolved in the plasma in the inlet and outlet stream, respectively. In blood oxygenation it is more common to use the oxygen partial pressure than the dissolved oxygen concentration. Thus Eq. 50 may be written as

$$K = \frac{Q}{A}\int_{P_{O_2,I}}^{P_{O_2,O}} \frac{\beta(Ht/100)(dS/dP_{O_2}) + \alpha}{(P^*_{O_2} - P_{O_2})} dP_{O_2} \quad (51)$$

where $P_{O_2,I}$, $PO_{2,O}$, and $P^*_{O_2}$ are the inlet and outlet oxygen partial pressures that would be in equilibrium with the oxygen in the blood and the oxygen partial pressure in the gas phase, respectively. dS/dP_{O_2} can be obtained by differentiating Eq. 26.

Finally, the overall average mass-transfer coefficient in the absence of the reaction between oxygen and hemoglobin may be calculated from

$$K_0 = \frac{Q}{A}\int_{P_{O_2,I}}^{P_{O_2,O}} \frac{\beta(Ht/100)(dS/dP_{O_2}) + \alpha}{E(P^*_{O_2} - P_{O_2})} dP_{O_2} \quad (52)$$

The Sherwood number for flat-sheet and hollow-fiber BOs is defined using Eqs. 6 and 13, respectively, where the mass-transfer coefficient in the absence of the reaction between oxygen and hemoglobin K_0 is used.

Numerical determination of enhancement factor

The mass-transfer coefficient of oxygen in the absence of the reaction between oxygen and hemoglobin, given by Eq. 52, was calculated numerically using the four-stage Runge–Kutta integration method by dividing the BO into a number of cells. At each integration point, the enhancement factor was calculated from Eq. 46. In Eq. 46 it is assumed that at the surface of the membrane in contact with blood, the oxygen concentration in the blood is in equilibrium with the gas phase. Thus $[O_2]_0$ at the inlet and outlet of the BO may be calculated from the oxygen partial pressure in the gas phase entering and exiting the BO. The gas-phase oxygen partial pressure is assumed to vary linearly between the inlet and outlet concentrations. The solubility of oxygen in blood α was taken as 9.46×10^{-6} mol m^{-3} Pa (Matsuda and Sakai, 2000). The inlet and outlet oxygen partial pressures in blood were determined experimentally and assumed to vary linearly along the flow direction. Therefore the degree of oxygen saturation S may be calculated using Eq. 26 for each integration point. The concentration of nonoxygenated hemoglobin, $[Hb]_\delta$, may be calculated from

$$[Hb]_\delta = (1 - S)[Hb]_t \quad (53)$$

The hematocrit (Ht) was measured experimentally and may be related to the hemoglobin concentration [Hb] by (Vaslef et al., 1994)

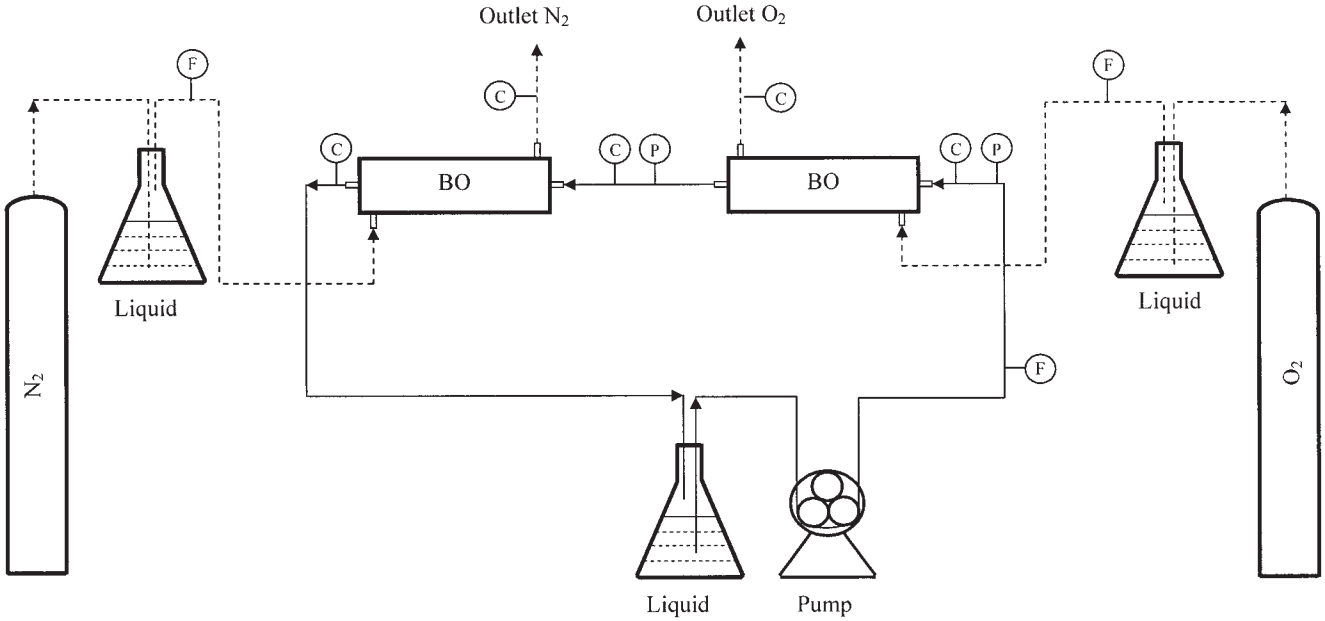

Figure 3. Experimental setup.

$$[\text{Hb}]\ (\text{mol m}^{-3}) = 0.408\text{Ht}\ (\%) \tag{54}$$

The diffusivity of oxygen in bovine blood was estimated using the following equation (Katoh and Yoshida, 1972)

$$D_{O_2} = (2.13 - 0.0092\text{Ht}) \times 10^{-9} \tag{55}$$

where D_{O_2} is in $m^2\ s^{-1}$. Dissolved oxygen can exist only in the blood plasma. Consequently, the diffusivity of oxygen must depend on the hematocrit of the blood.

Hemoglobin exists inside the red blood cells. Thus the red blood cell diffusivity was used as the diffusivity of oxygenated and nonoxygenated hemoglobin. The Brownian diffusivity of red blood cells is very low, $6.8 \times 10^{-14}\ m^2\ s^{-1}$ (Freitas, 1999). However, the diffusivity of red blood cells is significantly enhanced by the rotation and deformation of the cells. The effective diffusivity of red blood cells is given by (Freitas, 1999)

$$D_e = D + 0.25R_{rbc}^2\dot{\gamma} \tag{56}$$

where D_e is the effective diffusivity and R_{rbc} is the radius of a red blood cell, which is approximated by a sphere. As can be seen, the effective diffusivity is affected by shear rate. At a typical blood shear rate of around $500\ s^{-1}$, the effective diffusivity of the red blood cells is about $10^{-9}\ m^2\ s^{-1}$. Thus a red blood cell diffusivity of $10^{-9}\ m^2\ s^{-1}$ is used here.

Experimental Methods

The experimental setup used for the blood analogue fluids is shown in Figure 3. Table 2 summarizes the fluids tested. The liquid stream was pumped from the feed reservoir using a Masterflex peristaltic pump (Cole–Parmer, Vernon Hills, IL). Having passed through a rotameter, the liquid stream was introduced into the first BO. The gas phase to the first BO consisted of pure oxygen. Before flowing into the BO, the oxygen was saturated by bubbling it through a sample of the liquid stream. The liquid stream leaving the first BO was then fed into the second BO. In this device the sweep gas consisted of nitrogen saturated by the liquid stream. Thus the liquid stream was oxygenated in the first BO and deoxygenated in the

Table 2. Details of Newtonian and Non-Newtonian Blood Analogue Fluids and Bovine Blood*

System	Composition (Volume %)	Comments
Newtonian blood analogue systems: water (W)–glycerol (G) mixtures	100W, 95W:5G, 90W:10G, 80W:20G, 70W:30G, 60W:40G, 50W:50G	Tabulated viscosity data (Weast, 1974)
Non-Newtonian blood analogue systems: water (W)–glycerol (G)–xanthan (X) mixtures	Non-Newtonian blood analogue fluid 1: 59.9925W:40G:0.0075X	$\tau = 0.022\dot{\gamma}^{0.79}$
	Non-Newtonian blood analogue fluid 2: 59.96W:40G:0.04X	$\tau = 0.110\dot{\gamma}^{0.59}$
	Non-Newtonian blood analogue fluid 3: 49.925W:50G:0.075X	$\tau = 0.262\dot{\gamma}^{0.51}$
Bovine blood	25% Hematocrit	$\tau = 0.00709\dot{\gamma}^{0.73}$
	30% Hematocrit	$\tau = 0.01031\dot{\gamma}^{0.78}$
	35% Hematocrit	$\tau = 0.01396\dot{\gamma}^{0.63}$

*The viscosity of the Newtonian blood analogue fluids was determined from published values. Power-law constants m and n were determined experimentally for the non-Newtonian blood analogue fluids. Power-law constants for bovine blood were determined from published correlations (Barnes et al., 1993; Zydney et al., 1991).

Table 3. Oxygenators Tested

Oxygenator	Membrane	Comments
Cobe VPCML Plus	A flat-sheet microporous polypropylene membrane (thickness 50 ± 5 μm) is crimped to form blood channels 230 μm thick.	Consists of two compartments, one with a membrane surface area of 0.4 m^2 and the other 0.85 m^2. In these experiments each compartment was tested separately.
Cobe CML Duo	A flat-sheet microporous polypropylene membrane (thickness 50 ± 5 μm) is crimped to form blood channels 160 μm thick.	Two oxygenation compartments (each 1.3 m^2) are linked in series. Experiments were conducted using membrane surface areas of 1.3 and 2.6 m^2.
Cobe Optima XP	There are 14,500 microporous polypropylene hollow fibers (200 ± 30 μm inside diameter, 300 ± 30 μm outside diameter). Total surface area, equivalent diameter, and void fraction are 1.9 m^2, 480 μm, and 0.615, respectively.	Liquid fluids flow outside the fibers, whereas gases flow in the fiber lumen.
Cobe Optimin	There are 7000 microporous polypropylene hollow fibers (200 ± 30 μm inside diameter, 300 ± 30 μm outside diameter). Total surface area, equivalent diameter, and void fraction are 1.0 m^2, 516 μm, and 0.633, respectively.	Liquid fluids flow outside the fibers, whereas gases flow in the fiber lumen.

second BO. The outlet from the second BO was returned to the feed reservoir. Two gas flow rates, 0.81 and 2.1 L min^{-1}, were tested. Liquid flow rates ranged from 0.5 to 11 L min^{-1}.

The oxygen concentration of the liquid stream flowing into and out of the first BO and out of the second BO was measured using oxygen electrodes (Microelectrodes, Bedford, NH). The oxygen concentration in the gas streams leaving both BOs was also measured using Microelectrodes oxygen electrodes. The oxygen concentration in the inlet gases was either 100% (oxygen) or 0% (nitrogen). The liquid side pressure into and out of the first BO was measured using pressure transducers (Omega Engineering, Stamford, CT). The liquid stream flowing back to the feed reservoir from the second BO was at atmospheric pressure.

Literature values were used for the kinematic viscosity of the glycerol–water mixtures (Weast, 1974). Non-Newtonian blood analogue fluids were rheologically characterized before testing. The power-law parameters m and n for the non-Newtonian fluids were determined using a Brookfield Synchro-Letric Viscometer and LV spindle set (Brookfield Engineering Laboratories, Middelboro, MA). Rotation speeds ranged from 5 to 100 rpm. Experiments using bovine blood were conducted at Cobe Cardiovascular (Arvada, CO) using blood from two different animals. The pH and temperature of the blood were 7.4 and 37°C, respectively.

Flat-sheet and hollow-fiber BOs were obtained from Cobe Cardiovascular. Details are given in Table 3. Two flat-sheet BOs (Cobe VPCML Plus and Cobe Duo) were tested. The VPCML Plus contains two separate membrane compartments (0.4 and 0.85 m^2) for oxygenation. Each compartment was tested separately. The CML Duo also consists of two separate membrane compartments (each 1.3 m^2) for blood oxygenation. The Duo was tested using a single compartment and with both compartments combined. Consequently, four different membrane surface areas (0.4, 0.85, 1.3, and 2.6 m^2) were tested.

Two hollow-fiber BOs were tested. The Cope Optima XP contains 14,500 hollow fibers, whereas the Optimin contains 7000 hollow fibers (200 μm ID). In these BOs the hollow fibers are woven together to form a mat. The BOs were tested as designed: the liquid phase flowed outside the fibers, whereas the gas phase flowed inside the fibers.

All experiments were repeated at least three times. Average experimental results are presented in Figures 4–7. Error bars are used to indicate the variability in repeated experimental results. Where error bars are not shown, the actual symbol represents the variability in the reading.

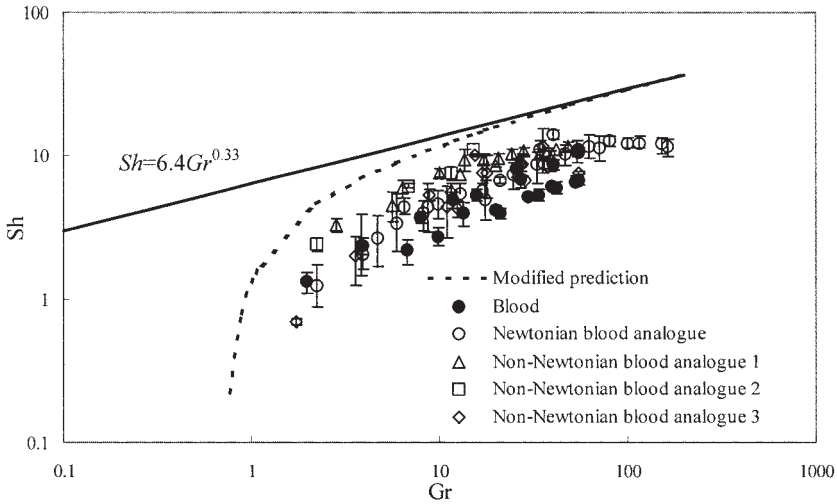

Figure 4. Variation of Sherwood number with Graetz number for flat-sheet BOs.

Non-Newtonian blood analogue fluids 1–3 are given in Table 2.

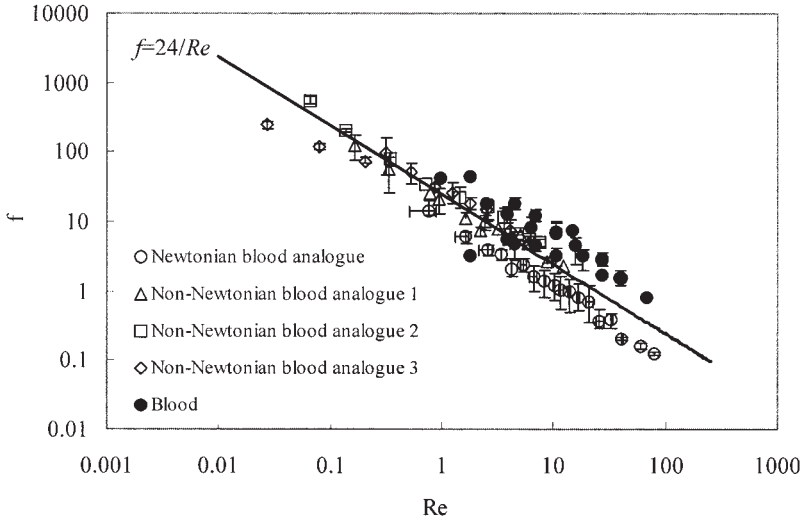

Figure 5. Variation of friction factor with Reynolds number for flat-sheet BOs.

Non-Newtonian blood analogue fluids 1–3 are given in Table 2.

Results

Experimentally determined power-law parameters for the non-Newtonian blood analogue fluids and bovine blood are given in Table 2. As can be seen, for the glycerol–water–xanthan gum mixtures, the higher the concentration of xanthan gum the greater the shear-thinning of the fluid. This is expected because it is the presence of xanthan gum that makes the fluid shear-thinning.

The power-law parameters for bovine blood were determined using literature correlations (Barnes et al., 1993; Zydney et al., 1991). Although these correlations were developed for human blood, previous investigators (Vaslef et al., 1994) showed that, under the operating conditions present during blood oxygenation, bovine blood is a very good substitute for human blood. Table 2 shows that the shear-thinning behavior of 25, 30, and 35% hematocrit bovine blood is approximately bracketed by the three non-Newtonian blood analogue fluids tested.

Figure 4 gives the variation of the Sherwood number with Graetz number for the flat-sheet BOs tested. For the Newtonian fluids the Sherwood and Graetz numbers were determined using Eqs. 6 and 7. The diffusivity of oxygen in the various glycerol–water mixtures was estimated from the Wilke–Chang equation (Wilke and Chang, 1955). Results for the four different membrane surface areas for oxygenation and deoxygenation at both gas flow rates are represented by open circles.

Open triangles, squares, and diamonds represent the results for the three different non-Newtonian blood analogue fluids. Results for the four different membrane surface areas for oxygenation and deoxygenation at both gas flow rates have been combined. The Sherwood and Graetz numbers were determined using Eqs. 6 and 22. The diffusivity of oxygen in the various glycerol–water–xanthan gum mixtures was estimated using the Wilke–Chang equation (Wilke and Chang, 1955). As can be seen by using the Graetz number, defined by Eq. 22, good agreement is obtained between the mass-transfer results for the Newtonian and non-Newtonian fluids.

Results for bovine blood are shown using filled circles. Results for bovine blood at three different hematocrits (25, 30, and 35%) for the four different membrane surface areas for oxygenation and deoxygenation at both gas flow rates have been combined. Figure 4 shows that the mass-transfer results for bovine blood are in agreement with the results obtained for the blood analogue fluids if the shear-thinning behavior of the blood and the enhancement factor arising from the oxygen hemoglobin reaction are taken into account. Although units of blood from different animals show considerable variability, this variability is not reflected here because blood from the same animal was used in Figures 4 and 5.

Equation 5 is represented by the solid line. As can be seen, for Graetz numbers > 10, the experimental data lie below but parallel to the theoretical prediction. However, at Graetz numbers < 10 the experimental and theoretical results deviate. The dashed curve is the prediction obtained if Eq. 4 is used to predict the mass-transfer coefficient. Before using Eq. 4, ε_0, the ratio of the standard deviation to the mean channel thickness, must be estimated. Goerke et al. (2002) showed that ε_0 is 0.06 for the flat-sheet BOs tested here. Using this value for ε_0 the dashed curve shown in Figure 4 is obtained. Equation 4 was derived by Goerke et al. (2002) by ignoring higher-order terms in ε_0. If the term containing ε_0^2 is not much smaller than 1, higher-order terms should be included. In Figure 4, Eq. 4 has been plotted beyond its range of applicability to demonstrate that it predicts the experimentally observed trend that at decreasing Graetz numbers the Sherwood number depends more strongly on Graetz number. As can be seen by accounting for polydispersity in the flow channels the agreement between the predicted and experimentally determined Sherwood numbers is improved.

The variation of the friction factor with Reynolds number is given in Figure 5. Open circles represent the results for the Newtonian blood analogue fluids. Equations 8 and 9 were used to determine the friction factor and Reynolds number, respectively. Results for the four different membrane surface areas have been combined.

Results for the three non-Newtonian blood analogue fluids

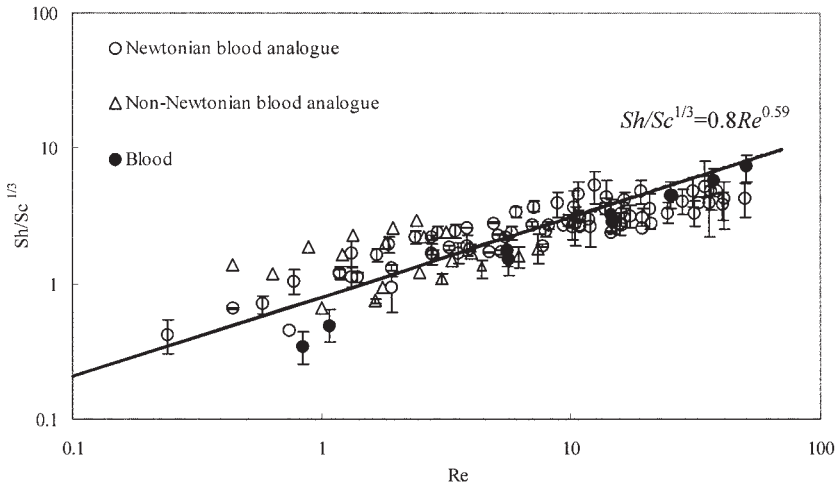

Figure 6. Variation of Sherwood number divided by the Schmidt number raised to the 1/3 power with Reynolds number for hollow-fiber BOs.

are represented by open triangles, squares, and diamonds, respectively. The results for bovine blood are given by filled circles. The friction factor and Reynolds numbers were determined using Eqs. 8 and 23, respectively. In Eq. 8 the average velocity of a power-law fluid u_p, calculated from Eq. 21, was used. Results for the four different membrane surface areas have been combined. The solid line represents the theoretical correlation given by Eq. 8.

Figure 5 indicates that Eq. 8 may be used to represents the experimental data, provided u_p and a generalized Reynolds number are used for shear-thinning fluids. Although bovine blood shows considerable variability, results shown here are for blood from a single animal. Consequently, the natural variability of bovine blood is not reflected in the results shown in Figure 5 and may explain why the majority of the results lie above the line represented by $f = \mathrm{Re}/24$.

Figures 6 and 7 give results for hollow-fiber BOs. Figure 6 shows the variation of the Sherwood number divided by the Schmidt number raised to the 1/3 power with Reynolds number. Results for the Newtonian blood analogue fluids are represented using open circles, whereas results for non-Newtonian blood analogue fluids are shown using open triangles. For the Newtonian blood analogue fluids the Schmidt, Sherwood, and Reynolds numbers were determined using Eqs. 12, 13, and 14, respectively. For the non-Newtonian blood analogue fluids the Sherwood, Reynolds, and Schmidt numbers were determined using Eqs. 13, 19, and 20, respectively. The mass-transfer correlation given by Eq. 11 is represented as a solid line. As described by Wickramasinghe et al. (2002a,b), Eq. 11 predicts the results for Newtonian and non-Newtonian blood analogue fluids.

Figure 6 shows that the mass-transfer results for bovine blood are also predicted using Eq. 11. These results are represented using filled circles. The Sherwood number was determined using Eq. 13, where the mass-transfer coefficient was divided by the enhancement factor (Eq. 46). Equations 19 and 20 were used to determine the Reynolds and Schmidt numbers, respectively. The results for both BOs for oxygenation and deoxygenation at both gas flow rates have been combined for the Newtonian and non-Newtonian blood analogue fluids and for bovine blood.

Figure 7 gives the variation of the friction factor with Reynolds number for flow across woven hollow fibers. The results for Newtonian blood analogue fluids are represented using open circles. The solid lines represent the two friction-factor correlations given by Eqs. 16 and 17. Wickramasinghe et al. (2002a) showed that these correlations successfully describe the variation of the friction factor for Newtonian fluids.

Results for the three non-Newtonian blood analogue fluids are represented by open triangles, squares, and diamonds. Results for bovine blood are represented by filled circles. In Eqs. 16 and 17 the average velocity of a power-law fluid u_p was calculated using Eq. 21. Figure 7 shows that Eqs. 16 and 17 successfully predict the variation of the friction factor for the non-Newtonian blood analogue fluids and for bovine blood. As was the case for Figures 4 and 5, blood from the same animal was used in Figures 6 and 7. Consequently, the natural variability of bovine blood is not represented in these figures.

Discussion

The experimental results for flat-sheet and hollow-fiber BOs indicate that the Sherwood number depends on the liquid flow rate but not the gas flow rate because results for both gas flow rates are indistinguishable. Thus, as expected, the liquid side concentration boundary layer represents the major resistance to mass transfer. This was observed by Goerke et al. (2002) for Newtonian fluids. Here we show the same is true for non-Newtonian blood analogue fluids as well as for bovine blood.

Figure 4 indicates that the actual rate of mass transfer is always less than predicted by the Lévêque solution. Goerke et al. (2002) discuss this observation in detail for Newtonian blood analogue fluids. The flat-sheet BOs studied here contain a screen in the blood channel that prevents the membrane layers from collapsing on top of each other. Areas of contact between the screen and the membrane surface are not available for mass transfer, resulting in the effective surface area for mass transfer being less than the actual membrane surface area

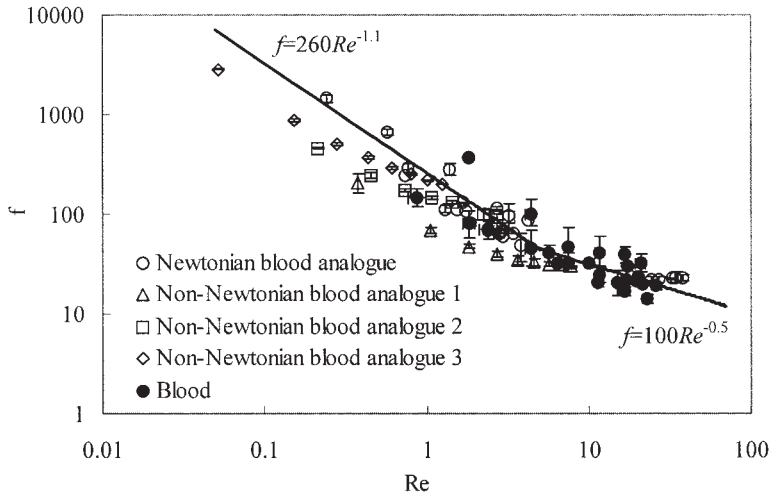

Figure 7. Variation of friction factor with Reynolds number for hollow-fiber BOs.

Non-Newtonian blood analogue fluids 1–3 are given in Table 2.

present. Thus the experimentally derived Sherwood numbers are less than those theoretically predicted for Graetz numbers > 10.

At Graetz numbers < 10, the experimentally determined Sherwood numbers are much lower than those predicted by the Lévêque solution. At low liquid flow rates slight variations in the blood flow channel thickness will lead to a lower gas transfer efficiency, attributed to channeling and bypassing of the liquid flow. By accounting for slight variations in the thickness of the flow channels, Goerke et al. (2002) were able to better predict the experimental results at lower flow rates. Here we show that previous mass-transfer results obtained for Newtonian blood analogue fluids are consistent with those obtained for non-Newtonian blood analogue fluids and bovine blood. The results for Newtonian blood analogue fluids obtained in earlier studies can show considerable deviation, especially at lower Graetz numbers, from the mass-transfer correlations that have been proposed (Wickramasinghe et al., 1992; Goerke et al., 2002). Our results here indicate that we obtain good agreement between these earlier experimental results for Newtonian blood analogue fluids and the results for non-Newtonian blood analogue fluids and bovine blood. Consequently results for oxygenation and deoxygenation of an experimentally simple system may be used to predict the rate of oxygen transfer to blood in a BO.

Figure 5 shows that the variation of the friction factor with Reynolds number, obtained for Newtonian blood analogue fluids by Goerke et al. (2002), is consistent with the results obtained in this study for non-Newtonian blood analogue fluids and bovine blood. The friction factor, unlike the mass-transfer coefficient, is insensitive to small variations in the thickness of the liquid flow channels. The strong dependency of the mass-transfer coefficient on slight variations in the thickness of the flow channels at low Graetz numbers arises from the fact that the mass-transfer coefficient depends on the logarithm of the oxygen concentration (Eq. 3).

For hollow-fiber BOs, Figure 6 shows that the mass-transfer results for all the fluids tested are in agreement with the experimental correlation given by Eq. 11. This correlation was developed by Wickramasinghe et al. (2002a) for Newtonian blood analogue fluids. Here we show that the mass-transfer results for bovine blood are in agreement with this experimentally derived correlation. The mass-transfer results for the oxygenation of deionized water may be used to predict the performance of hollow-fiber BOs in clinical use. Although this correlation was derived using three different BOs manufactured by Cobe, Wickramasinghe et al. (1992) noted that different commercially available BOs give similar performance.

The variation of the friction factor with Reynolds number for hollow-fiber BOs may be described by two different correlations. Figure 7 shows that at Reynolds numbers between 5 and 10, the slope of the friction factor vs. Reynolds number curve changes, suggesting the onset of boundary layer separation. Wickramasinghe et al. (2002a) derived these correlations based on experimental data for Newtonian blood analogue fluids. Here we show that the same correlations describe the results for non-Newtonian blood analogue fluids and for bovine blood.

Previous attempts to predict the gas-transfer efficiency for blood are summarized in Table 4. Spaeth (1973) summarized many of the early theoretical studies and described the various limiting conditions often considered. Before the use of microporous membranes, to improve the hemocompatibility of BOs, and avoid direct contact between blood and gas, a nonporous membrane was placed between the blood and gas phases of BOs (Clowes et al., 1956; Kolff and Balzer, 1956). Consequently, most of these early studies considered blood flowing inside nonporous hollow fibers or in nonporous rectangular channels.

Today BOs are designed to include passive mixing of the blood to disrupt the liquid side concentration boundary layer and thus increase the gas-transfer efficiency. In hollow-fiber BOs, the blood flows outside and across the fibers rather than inside the fibers. Thus the fibers themselves induce mixing of the blood. Consequently, earlier analyses that considered blood flow inside the fiber are of limited value. In the flat-sheet BOs studied here, the screen that is placed in the blood flow channel to prevent the flat-sheet membranes from collapsing on top of each other also induces mixing of the blood.

Mockros and Leonard (1985) considered blood flowing outside and across bundles of hollow fibers. A mass-transfer

Table 4. Previous Attempts to Predict the Gas Transfer Efficiency for Blood

BO Configuration	Main Assumptions	References
Flow inside tubes	Liquid flow consists of two zones; hemoglobin in the outer zone is fully oxygenated but not in the inner zone	Lightfoot (1968); Dorson et al. (1971)
Flow inside tubes	Solved continuity equation assuming laminar flow	Weisman and Mocckros (1967)
Flow inside rectangular channels	Solved continuity equation assuming laminar flow	Semby and Grimsrud (1974)
Flow across microporous hollow fibers	Used a modified diffusion coefficient to account for the reaction between oxygen and hemoglobin	Weissman and Mockros (1967, 1969); Mockros and Leonard (1985); Vaslef (1990); Vaslef et al. (1994); Rajasubramanian et al. (1997)
Flow across microporous hollow fibers	Determined a mass-transfer enhancement factor as a function of hematocrit	Matsuda and Sakai (2000); Kotoh and Yoshida (1972); Yoshida (1993)

correlation of the form given by Eq. 10 was assumed where $c = 1/3$, as predicted from analogous heat-transfer correlations. Because Eq. 10 applies to nonreactive systems it is essential to account for the enhancement to the mass-transfer coefficient that results from the reaction between oxygen and hemoglobin. In an earlier study, Weissman and Mockros (1967, 1969) considered the rate of gas transfer to blood flowing in laminar flow inside hollow fibers. Rearrangement of the continuity equation results in a parameter, $D/[1 + f(C)]$, where D is the diffusion coefficient of oxygen in blood, C is the concentration of dissolved oxygen in the blood, and $f(C)$ is a term to account for oxygen that binds to hemoglobin. It can be shown that $f(C)$ is proportional to the slope of the oxyhemaglobin saturation/dissociation curve (Eq. 26). The same parameter, defined as a modified diffusion coefficient, was used for flow across bundles of hollow fibers. This analysis has been used in many subsequent studies (Rajasubramanian et al., 1997; Vaslef, 1990; Vaslef et al., 1994).

In a recent study, Matsuda and Sakai (2000) considered oxygen transfer to blood flowing outside and across hollow fibers. They also assumed a mass-transfer correlation of the form given by Eq. 10, where $c = 1/3$. However, the authors used the Adair equation (Adair, 1925) rather than the Hill equation to describe the oxyhemoglobin saturation/dissociation curve. The Adair analysis assumes that oxygen binding to hemoglobin can be characterized by four successive equilibria. However, because the four heme units in the hemoglobin molecule do not independently react with O_2, the four macroscopic equilibrium constants do not represent four elementary steps. Further deviations between the predicted oxyhemoglobin saturation/dissociation curves given by the Hill and Adair analyses are minor (Antonini and Brunori, 1975).

Matsuda and Sakai (2000) used the enhancement factor described by Katoh and Yoshida (1972) and Yoshida (1993) to account for the enhancement to the mass-transfer coefficient arising from the reaction between oxygen and hemoglobin. These latter authors determined the rate of oxygen transfer to normal blood and to blood where the hemoglobin was inactivated by prior exposure to carbon monoxide. The mass-transfer enhancement factor was determined as a function of hematocrit. By fitting a curve to this data, an empirical expression was obtained for the variation of the enhancement factor with hematocrit.

The current study uses a very different approach. Here we assume film theory. The analysis presented by Olander (1960) and Huang and Kuo (1965) is then extended to account for the reaction stoichiometry given by the rate expression in Eq. 25. This rate expression is based on the Hill equation. The Adair equation could also be used, although there is little physical insight gained because the four successive equilibria do not represent four elementary reactions between oxygen and hemoglobin. Further, the form of the Hill equation is identical to the Freundlich–Langmuir isotherm, which is used frequently in adsorption studies.

Because the mass-transfer enhancement factor developed here is based on film theory it is valid for any BO design, providing film theory is appropriate. The enhancement factor may be used to compare mass-transfer data for blood and nonreactive blood analogue fluids where mass-transfer correlations other than Eqs. 5 and 11 are applicable. Further, we show that by defining generalized Reynolds, Schmidt, and Graetz numbers, the mass-transfer and friction-factor correlations derived for non-Newtonian blood analogue fluids may be used to predict the actual performance of a BO in clinical use.

The mass-transfer enhancement factor depends on the diffusivity of red blood cells. As the diffusivity of the red blood cells increases so does the mass-transfer enhancement factor. Here a diffusivity at 500 s^{-1} is used where the diffusivity of red blood cells is dominated by their shear-induced diffusivity. BO designs that maximize the diffusivity of red blood cells will display higher rates of gas transfer.

The mathematical expression for the mass-transfer enhancement factor in Eq. 46 is a consequence of assuming film theory. Mass-transfer enhancement factors may be determined using other theories such as penetration and surface renewal. However, because passive mixing of the blood is promoted in the design of BOs, a penetration depth would have to be assumed. In the case of surface renewal theory, it is likely that the residence time distribution for blood analogue fluids may be different from that of blood because of the presence of blood cells.

In this work we focus on oxygen transfer. For microporous-membrane BOs it is the transfer of oxygen rather than carbon dioxide that is limiting (Voorhees and Brian, 1996). Dividing the mass-transfer coefficient obtained from experiments with blood by the mass-transfer enhancement factor eliminates the effect of the oxygen hemoglobin reaction on the rate of mass transfer. Thus the blood results can now be compared to results obtained for nonreactive systems such as the oxygenation of deionized water.

The analysis presented here may be used to predict the level of oxygen saturation in blood using mass-transfer data from a simple experimental system such as the oxygenation/deoxygenation of water. For example, by using Eq. 46, the mass-transfer coefficient for the oxygenation/deoxygenation of water and the initial oxygen saturation of the blood, the outlet oxygen saturation of the blood can be determined. In addition by using generalized Reynolds, Schmidt, and Graetz numbers and the

average velocity for a shear-thinning fluid u_p, the shear-thinning behavior of blood is included in the mass-transfer and friction-factor correlations.

Conclusion

Mass-transfer and friction-factor correlations for flat-sheet and hollow-fiber BOs have been developed using Newtonian and non-Newtonian blood analogue fluids, and bovine blood. A mass-transfer enhancement factor based on film theory is proposed that can predict the oxygen saturation in blood based on results for nonreactive blood analogue fluids. The mass-transfer enhancement factor does not depend on assuming a particular form of the mass-transfer correlation. It is valid for any BO design where film theory is appropriate. For flat-sheet and hollow-fiber BOs good agreement is obtained between the results for nonreactive blood analogue fluids and bovine blood. Generalized Reynolds, Schmidt, and Graetz numbers, as well as an analogous velocity for power-law fluids, are defined to account for the shear-thinning behavior of blood.

Acknowledgments

Financial support for this work was provided by Cobe Cardiovascular (Arvada, CO), the Colorado Institute for Research in Biotechnology, and the National Science Foundation (CAREER Program Grant BES 9984095 and REU Program Grants EEC-9820545 and EEC-0139478). The authors acknowledge Aaron Goerke and John Leung for conducting some of the experiments.

Notation

a = empirical constant
a_1, a_2, a_3, a_4 = constants
A = membrane surface area
b = empirical constant
B = average half-thickness of the rectangular channels
c = empirical constant
C = concentration
C^* = oxygen concentration in the liquid in equilibrium with the gas phase
C_C = oxygen bound to hemoglobin
C_P = oxygen dissolved in plasma
$C_{P,I}$ = physically dissolved oxygen in plasma at the inlet of the BO
$C_{P,O}$ = physically dissolved oxygen in plasma at the outlet of the BO
ΔC = overall concentration difference
d_0 = diffusion coefficient
D_e = effective diffusivity of red blood cells
d_e = equivalent diameter
D = outside diameter of the hollow fibers
E = enhancement factor
f = friction factor
$f(C)$ = function to account for oxygen that binds to hemoglobin
Ht = hematocrit
J = flux
J_0 = oxygen flux in the absence of chemical reaction between oxygen and hemoglobin
k_0 = local mass-transfer coefficient in the boundary layer
K = overall average mass-transfer coefficient
K_D = reciprocal of the equilibrium constant
K_E = equilibrium constant
k = local mass-transfer coefficient in the absence of chemical reaction in the boundary layer
k_1 = forward rate constant
k_{-1} = backward rate constant
$\langle K \rangle$ = average mass-transfer coefficient for flow in polydisperse channels
L = length of rectangular channel
L_0 = length of hollow-fiber BO
m = power-law parameter
n = power-law parameter; measure of cooperativity between heme units in Eq. 24
N = total molar flux
P_{O_2} = oxygen partial pressure
$P_{O_2,I}$ = inlet oxygen partial pressure in equilibrium with the oxygen in the blood
$P_{O_2,O}$ = outlet oxygen partial pressure in equilibrium with the oxygen in the blood
$P^*_{O_2}$ = oxygen partial pressure in the gas phase
P_{50} = oxygen partial pressure at 50% hemoglobin saturation
ΔP = pressure drop
Q = fluid flow rate
R_{rbc} = radius of red blood cell assumed to be spherical
S = degree of oxygen saturation
t = time
u = liquid velocity
u_p = average velocity of non-Newtonian fluid
x = distance variable

Greek letters

α = physical solubility of oxygen in blood
β = maximum amount of oxygen combined with a unit volume of hemoglobin
ε = void fraction of a BO
ε_0 = standard deviation divided by the mean of the distribution of channel thickness
ρ = liquid density
ν = kinematic viscosity of Newtonian fluids
ν_p = kinematic viscosity of non-Newtonian fluid
τ = shear stress
$\dot{\gamma}$ = shear rate
δ = thickness of boundary layer

Dimensionless terms

Gr = Graetz number, $(4B)^2u/(DL)$
Gr_p = generalized Graetz number for power-law fluids, $(4B)^2u_p/(DL)$
Re = Reynolds number, $u(4B)/\nu$, ud_e/ν
Re_p = generalized Reynolds number for power-law fluids, $u_p(4B)/\nu_p$, u_pd_e/ν_p
Sc = Schmidt number, ν/D
Sc_p = generalized Schmidt number for power-law fluids, ν_p/D
Sh = Sherwood number, $K(4B)/D$, Kd_e/D

Subscripts

e = equilibrium; effective
Hb = hemoglobin
$Hb(O_2)_n$ = oxyhemoglobin
I = inlet
O = outlet
O_2 = oxygen
p = power law
t = total

Literature Cited

Adair, G. S., "The Hemoglobin System," *J. Biol. Chem.*, **63**, 493 (1925).
Altman, P. L., and D. S. Dittmer, *Blood and Other Body Fluids*, Federation of American Societies for Experimental Biology, Bethesda, MD (1971).
Antonini, E., and M. Brunori, "Hemoglobin and Methemoglobin," *The Red Blood Cell*, 2nd Ed., Vol. II, D. M. Surgenor, Ed., Academic Press, New York (1975).
Barnes, H. A., J. F. Hutton, and K. Walters, *An Introduction to Rheology*, 3rd ed., Elsevier, New York (1993).
Baurmeister, U., "Multilayer Hollow Fiber Wound Body," U.S. Patent No. 4 940 617 (1990).
Baurmeister, U., "Multilayer Hollow Fiber Wound Body," U.S. Patent No. 5 143 312 (1992).

Bellhouse, B. J., F. H. Bellhouse, C. M. Curl, T. I. MacMillan, A. J. Gunning, E. H. Spratt, S. B. MacMurray, and J. M. Nelems, "High-Efficiency Membrane Oxygenator and Pulsatile Pumping System, and Its Application to Animal Trials," *Trans. Am. Soc. Artif. Intern. Organs*, **19**, 72 (1973).

Bird, R. B., W. E. Stewart, and E. N. Lightfoot, *Transport Phenomena*, 2nd ed., Wiley, New York (2001).

Bludszuweit, C., "Evaluation and Optimization of Artificial Organs by Computational Fluid Dynamics," *Proc. of the 1997 ASME Fluids Eng. Div. Summer Meeting*, Vancouver, British Columbia, Canada (June 22–26, 1997).

Brookshier, K. A., and J. M. Tarbell, "Evaluation of Transparent Blood Analogue Fluids—Aqueous Xanthan Gum Glycerin," *Biorheology*, **30**, 107 (1993).

Chien, S., S. Usami, H. M. Taylor, J. L. Lundberg, and M. I. Gregersen, "Effects of Hematocrit and Plasma Proteins on Human Blood Rheology at Low Shear Rates," *J. Appl. Physiol.*, **21**, 81 (1966).

Clowes, G. H. A., A. L. Hopkins, and W. E. Neville, "An Artificial Lung Dependent upon Diffusion of Oxygen and Carbon Dioxide through Plastic Membranes," *J. Thorac. Surg.*, **32**, 630 (1956).

Cussler, E. L., *Diffusion: Mass Transfer in Fluid Systems*, 2nd ed., Cambridge Univ. Press, New York (1997).

Darby, R., *Chemical Engineering Fluid Mechanics*, Marcel Dekker, New York (1996).

Dittmer, D. S., and R. M. Grebe, *Handbook of Circulation*, W. B. Saunders Co., Philadelphia, PA (1959).

Dorson, W. J., Jr., K. G. Larsen, R. J. Elgas, and M. E. Voorhees, "Oxygen Transfer to Blood: Data and Theory," *Trans. Am. Soc. Artif. Intern. Organs*, 17, 309 (1971).

Freitas, R. A., Jr., *Nanomedicine, Vol. 1: Basic Capabilities*, Landes Bioscience, Austin, TX (1999).

Gartner, M. J., C. R. Wilhelm, K. L. Gage, M. C. Fabrizio, and W. R. Wagner, "Modeling Flow Effects on Thrombotic Deposition in a Membrane Oxygenator," *Artif. Organs*, **24**, 29 (2000).

Goerke, A. R., J. Leung, and S. R. Wickramasinghe, "Mass and Momentum Transfer in Blood Oxygenators," *Chem. Eng. Sci.*, **57**, 2035 (2002).

Goldstick, T. K., "Oxygen Transport," *Engineering Principles in Physiology*, Vol. 2, J. H. U. Brown, and D. S. Gann, Eds., Academic Press, New York (1973).

Goodin, M. S., E. J. Thor, and W. S. Haworth, "Use of Computational Fluid Dynamics in the Design of the Avecor Affinity Oxygenator," *Perfusion*, **9**, 217 (1994).

Graetz, L., "Ueber die Wärmeleitungsfähigkeit von Flüssigkeiten," *Ann. Phys. Chem.*, **18**, 79 (1883).

Graetz, L., "Ueber die Wärmeleitungsfähigkeit von Flüssigkeiten," *Ann. Phys. Chem.*, **25**, 337 (1885).

Hill, A. V., "The Possible Effects of the Aggregation of the Molecules of Hemoglobin on its Dissociation Curves," *J. Physiol.*, **XL**, IV (1910).

Huang, C.-J., and C.-H. Kuo, "Mathematical Models for Mass Transfer Accompanied by Reversible Chemical Reaction," *AIChE J.*, **11**, 901 (1965).

Katoh, S., and F. Yoshida, "Rates of Absorption of Oxygen into Blood under Turbulent Conditions," *Chem. Eng. J.*, **3**, 276 (1972).

Kolff, W. J., and R. Balzer, "The Artificial Coil Lung," *Trans. Am. Soc. Artif. Intern. Organs*, **1**, 39 (1956).

Lévêque, M. A., "Les Lois de la Transmission de Chaleur par Convection," *Ann. Mines*, **13**, 201 (1928).

Lightfoot, E. N., "Low-Order Approximations for Membrane Blood Oxygenators," *AIChE J.*, **14**, 669 (1968).

Liu, Z., *Methods for Studying Proteins and Enzymes*, Academic Press, Beijing, China (1989).

Matsuda, N., and K. Sakai, "Blood Flow and Oxygen Transfer Rate of an Outside Blood Flow Membrane Oxygenator," *J. Membr. Sci.*, **170**, 153 (2000).

Mockros, L. F., and R. Leonard, "Compact Cross-Flow Tubular Oxygenators," *Trans. Am. Soc. Artif. Intern. Organs*, **31**, 628 (1985).

Nernst, W., "Theorie der Reaktionsgeschwindigkeit in heterogenen Systemer," *Z. Phys. Chem.*, **47**, 52 (1904).

Olander, D. R., "Simultaneous Mass Transfer and Equilibrium Chemical Reaction," *AIChE J.*, **6**, 233 (1960).

Rajasubramanian, S., K. D. Nelson, P. Shastri, A. Constantinescu, P. Kulkarni, M. E. Jessen, and R. C. Eberhart, "Design of an Oxygenator with Enhanced Gas Transfer Efficiency," *ASAIO J.*, **43**, M710 (1997).

Ranney, H. M., and V. Sharma, "Structure and Function of Hemoglobin," *Williams Hematology*, 6th ed., E. Beutler, M. A. Lichtman, B. S. Coller, T. J. Kipps, and U. Seligsohn, Eds., McGraw Hill, New York (2001).

Semby, L., and L. Grimsrud, "Theoretical Investigation of Mass Transfer in Membrane Oxygenators," *Med. Biol. Eng.*, **12**, 698 (1974).

Shah, R. K., and A. L. London, "Thermal Boundary-Conditions and Some Solutions for Laminar Duct Flow Forced-Convection," *J. Heat Trans.*, **96**, 159 (1974).

Sirkar, K. K., "Other New Membrane Processes," *Membrane Handbook*, W. S. W. Ho and K. K. Sirkar, Eds., Van Nostrand Reinhold, New York (1992).

Spaeth, E. E., "Blood Oxygenation in Extracorporeal Devices: Theoretical Considerations," *CRC Crit. Rev. Bioeng.*, **1**, 383 (1973).

Suzuki, M., *Adsorption Engineering*, Kodansha, Tokyo, Japan (1990).

Thurston, G. B., "Rheological Parameters for the Viscosity, Viscoelasticity and Thixotropy of Blood," *Biorheology*, **16**, 149 (1979).

Vaslef, S. N., "Analysis and Design of an Intravascular Lung Assist Device," PhD Thesis, Northwestern University, Evanston, IL (1990).

Vaslef, S. N., L. F. Mockros, R. W. Anderson, and R. J. Leonard, "Use of a Mathematical Model to Predict Oxygen Transfer Rates in Hollow Fiber Membrane Oxygenators," *ASAIO J.*, **40**, 990 (1994).

Voorhees, M. E., and B. F. Brian III, "Blood Gas Exchange Devices," *Int. Anesthesiol. Clin.*, **34**, 29 (1996).

Weast, R. C., *CRC Handbook of Chemistry and Physics*, 55th ed., CRC Press, Cleveland, OH (1974).

Weissman, M. H. and L. F. Mockros, "Oxygen Transfer to Blood Flowing in Round Tubes," *J. Eng. Mech. Div.–ASCE*, **94**, 225 (1967).

Weissman, M. H., and L. F. Mockros, "Oxygen and Carbon Dioxide Transfer in Membrane Oxygenators," *Med. Biol. Eng.*, **7**, 169 (1969).

Wickramasinghe, S. R., J. D. Garcia, and B. Han, "Mass and Momentum Transfer in Hollow Fibre Blood Oxygenators," *J. Membr. Sci.*, **208**, 247 (2002a).

Wickramasinghe, S. R., C. M. Kahr, and B. Han, "Mass Transfer in Blood Oxygenators Using Blood Analogue Fluids," *Biotechnol. Prog.*, **18**, 867 (2002b).

Wickramasinghe, S. R., M. J. Semmens, and E. L. Cussler, "Mass-Transfer in Various Hollow Fiber Geometries," *J. Membr. Sci.*, **69**, 235 (1992).

Wilke, C. R., and P. Chang, "Correlation of Diffusion Coefficients in Dilute Solutions," *AIChE J.*, **1**, 264 (1955).

Yang, L. and P. Chen, "Chitosan/Coarse Filter Paper Composite Membrane for Fast Purification of IgG from Human Serum," *J. Membr. Sci.*, **205**, 141 (2002).

Yang, M.-C., and E. L. Cussler, "Designing Hollow-Fiber Contactors," *AIChE J.*, **32**, 1910 (1986).

Yoshida, F., "Prediction of Oxygen Transfer Performance of Blood Oxygenators," *Artif. Organs Today*, **2**, 237 (1993).

Zhang, Q., and E. L. Cussler, "Microporous Hollow Fibers for Gas-Absorption: I. Mass-Transfer in the Liquid," *J. Membr. Sci.*, **23**, 321 (1985a).

Zhang, Q., and E. L. Cussler, "Microporous Hollow Fibers for Gas-Absorption: II. Mass-Transfer Across the Membrane," *J. Membr. Sci.*, **23**, 333 (1985b).

Zydney, A. L., J. D. Oliver, and C. K. Colton, "A Constitutive Equation for the Viscosity of Stored Red-Cell Suspensions—Effect of Hematocrit, Shear Rate, and Suspending Phase," *J. Rheol.*, **35**, 1639 (1991).

Manuscript received Apr. 19, 2003, and revision received Jun. 6, 2004.